Primitive Pressure-Velocity Code for the Computation of Strongly Swirling Flows

David G. Lilley*
The University of Arizona, Tucson, Ariz.

As an aid to economical design and operation of combustion systems, a primitive pressure-velocity finite difference code has been developed to predict strongly swirling inert and reacting turbulent flow. The method and program involve a staggered grid system for axial and radial velocities, a line relaxation technique for efficient solution of the equations, and a two-equation k-ϵ turbulence model, together with a simple one-step chemical reaction model based on eddy-breakup concepts. Computations show the interesting effects of swirl on jet growth, entrainment, and decay, and flame size, shape, and combustion intensity, as well as the occurrence of a central toroidal recirculation zone at high degrees of swirl.

Nomenclature

a	= apparent origin distance, coupling coefficient
C	= contribution to cell surface intergal
C,U,V	= control cell columes for ϕ, u, v
c	= specific heat, constant
D	= chamber diameter
d	= nozzle diameter
E,P	= Arrhenius constants
fu,ox,pr	= fuel, oxidant, product
G	= axial flux of momentum, k = generation term
g	= mean square fluctuating component of fuel concentration
H	= heat of combustion
h	= stagnation enthalpy
I,J	= mesh point
i	= stoichiometric ratio
J	= turbulent flux vector
k	= kinetic energy of turbulence
M	= mean mixture molecular weight
m	= time-mean chemical mass fraction
$\dot{m}_{net}$	= net outflow of mass from cell
Pe	= cell Peclet number
p	= time-mean pressure
R	= universal gas constant, mass rate of creation per unit volume, residual source
S	= swirl number $= 2G_\theta/(G_x d)$, source term (with subscript)
S_P, S_U	= components of linearized source term
T	= time-mean temperature
$v=(u,v,w)$	= time-mean velocity (in x,r,θ directions)
x,r,θ	= axial, radial, polar coordinates
Γ	= turbulent exchange coefficient
Δ	= mean-flow rate of strain tensor
δx	= axial distance between two neighboring mesh points
ϵ	= turbulence energy dissipation rate
μ	= turbulent viscosity
ρ	= time-mean density
σ	= Prandtl-Schmidt number
τ	= turbulent stress tensor
ϕ	= swirl vane angle, dependent variable
∇	= vector differential operator

Superscripts

old	= last iterate value
*	= preliminary u,v, and p field based on estimate pressure field p^*
′	= correction value to u^*, v^*, p^* to get u,v,p

Subscripts

EBU	= eddy-breakup model
fu, ox, pr	= fuel, oxidant, product (including inerts)
h	= enthalpy equation, relating to hub
j	= jth species equation
m	= maximum value at a particular axial station
n,s,e,w	= north, south, east, west faces of cell
o	= value at orifice of jet
P,N,S,E,W	= point, north, south, east, west neighbors
p	= constant pressure
rx, etc.	= rx component of second-order tensor, etc.
x,θ	= direction x,θ
ϕ	= dependent variable

Presented as Paper 75-872 at the AIAA 8th Fluid and Plasma Dynamics Conference, Hartford, Conn., June 16-18, 1975; submitted July 10, 1975; revision received Nov. 5, 1975.

Index categories: Jets, Wakes, and Viscid-Inviscid Flow Interactions; Reactive Flows; Combustion in Gases.

*Associate Professor, Dept. of Chemical Engineering. Member AIAA.

I. Introduction

A. The Phenomenon

SWIRL is used extensively in combustion systems where, in the case of a gas turbine combustion chamber for example, the strong swirling vortex region in the primary zone helps to meet many of the performance requirements, largely at the expense of pressure loss. Designers are aided by experiments, but as an alternative to them economical design and operation can be greatly facilitated by the availability of prior predictions of the flowfield, obtained via the use of a mathematical model incorporating a numerical prediction procedure. Such work combines the rapidly developing fields of theoretical combustion aerodynamics and computational fluid dynamics and its improvement and use will significantly reduce the cost of experimental development programs.

Experimental studies[1] show that swirl has large-scale effects on flowfields: jet growth, entrainment, and decay (for inert flows) and flame size, shape, stability, and combustion intensity (for reacting flows) being affected by the degree of swirl imparted to the flow. This is characterized by the swirl number S, which is a nondimensional number representing the axial flux of swirl momentum divided by the axial flux of axial momentum times equivalent nozzle radius, and the effect of swirl on the flow is related to this number. Strongly swirling flows (approximately $S>0.6$) possess sufficient radial and axial pressure gradients to cause a central toroidal recirculation zone, which is not observed at weaker degrees of swirl. This paper is concerned with the simulation and solution of these strongly swirling flows.

B. The Problem

The swirl strength determines the degree of upstream influence and the swirl number S measures this degree of swirl. The flow classification of parabolic (boundary-layer type with a single predominant direction – weak swirl $S<0.4$) or elliptic (recirculating type with upstream influence – strong swirl $S>0.6$) governs the type of boundary conditions required and solution method. Marching methods are appropriate for the former, relaxation methods for the latter.[2,3] Most combustion systems exhibit recirculation. The presence of swirl and transverse injection of dilutant air causes a toroidal vortex to form in the middle of the combustion chamber, in addition to any corner recirculation zone near the entrance which may be provoked by the sudden expansion of the cross-sectional area.

A mathematical solution of the flowfield of interest should provide results, if possible more cheaply, quickly, and correctly than possible by other means (for example, experiments on real-life systems or models). In order to achieve this, the model should simulate the flow in all its important respects (geometry, boundary conditions, physical properties of gases, turbulence, combustion, etc.) and provide a means whereby the governing equations may be solved. Mathematical models of steadily increasing realism and refinement are now being developed, both in the dimensionality of the model (together with the computational procedures) and in problems associated with the simulation of the physical processes occurring. Clearly there are two areas of difficulty: the simulation and the solution. Consideration is given here to a new primitive, pressure-velocity variable, finite difference code which has been developed to predict 2-D axisymmetric strongly swirling, inert and reacting, turbulent flows.

C. Previous Work

The author has previously been engaged on the simulation and solution of various types of swirling flows – parabolic and elliptic, inert and reacting, free and confined.[3-8] The simulation, via turbulence and reaction models, is touched on here only obliquely as it is discussed at length in Refs. 6-8. Attention is given primarily to the computational problem of solving the set of strongly-coupled elliptic governing equations via a relaxation procedure. One has the choice of a stream function-vorticity or primitive pressure-velocity approach. Whereas the former approach, used in the 1968 computer program from Imperial College[9] for example, reduces by one the number of equations to be solved and eliminates the troublesome pressure (at the expense of trouble with the vorticity equation), the preferred approach now is SIMPLE (mnemonic for *s*emi-*i*mplict *m*ethod for *p*ressure *l*inked *e*quations), which focuses attention directly on the latter variables.[10-12] It possesses many advantages: it can be used for 3-D as well as 2-D problems, it can handle compressible and time-dependent problems as well as incompressible steady ones, and boundary conditions and variable properties are more accurately and realistically handled. The work here is developed immediately on this new technique, the basic ideas of which had been embodied into the 1974 Imperial College TEACH (*t*eaching *e*lliptic *a*xisymmetric *c*haracteristics *h*euristically) computer program.[12]

Steady 2-D elliptic flows are akin to the final state of steady 3-D developing boundary layers and the final state of unsteady 2-D flows. There is a large literature on these, usefully digested in the references.[13,14] The papers most relevant to the present work are those by Harlow and co-workers,[15,16] Chorin[17] and Spalding and co-workers,[10-12,18,19] the work described here incorporates the following:

1) A finite difference procedure is used in which the dependent variables are the velocity components and pressure.

2) The pressure is deduced from an equation which is obtained by the combination of the continuity equation and the momenta equations (yielding a new form of what is known in the literature as the Poisson equations for pressure).

3) The idea is present at each iteration of a first approximation to the solution followed by a succeeding correction.

4) The procedure incorporates displaced grids for the axial and radial velocities, u and v which are placed between the nodes where pressure p and other variables are stored.

5) An implicit line-by-line relaxation technique is employed in the solution procedure (requiring a tridiagonal matrix to be inverted in order to update a variable at all points along a column).

D. Outline of the Paper

The paper presents recent work in the finite difference solution, via a new primitive pressure-velocity variable finite difference code, of 2-D swirling inert and reacting turbulent recirculating flows. Whereas the principal interest is on application to gas turbine combustors, the emphasis here is on the free or confined flow downstream of sudden expansions of the cross-sectional flow area. Basic equations are presented and molded into a common form in Sec. II, but the simulation of turbulence and chemical reaction, which has been discussed at length quite recently,[6-8] takes a minor role here. Governing general strongly swirling flows perhaps with recirculation, the equations are elliptic in character and together with this simualtion problem is the necessity to solve the equations; a lengthly numerical relaxation method is appropriate.

All aspects of the solution procedure are then dealt with in Sec. III via discussion of the grid system, control volumes, finite difference equations, boundary conditions, and solution procedure. The computer program solves directly for the primitive pressure and velocity variables, unlike a previous method[7] which obtains these by way of stream function and vorticity. In addition the u and v velocities are positioned between the nodes where p and other variables are stored and the combination of staggered grid and a line relaxation method leads to rapid solution. By this means it is possible to predict the major features of strongly swirling flows and, as examples of current predictive capability, two sets of computations are included in Sec. IV. The Conclusions section summarizes the achievements.

II. Theoretical Model

A. Governing Equations

The turbulent flux (Reynolds) equations of conservation of mass, momentum, stagnation enthalpy h, chemical specie mass fractions m_j, turbulence energy k, and turbulence dissipation rate ϵ, which govern the 2-D steady flow of turbulent chemically-reacting multicomponent mixtures, may be taken as previously.[7] These transport equations are all similar and contain terms for the convection and diffusion (via turbulent flux terms) and source S_ϕ of a general variable ϕ (which contains terms describing the generation (creation) and consumption (dissipation) of ϕ). Deferring their presentation until they are put in a common form, Eq. (11), if they are to be solved for time-mean pressure p, velocity v, temperature T and chemical specie mass fractions m_j, then the further thermodynamic unknowns (density ρ, stagnation enthalpy h and the mass rates of creation of species j per unit volume R_j) and turbulent flux unknowns (turbulent stress tensor τ and turbulence flux vectors J_ϕ for transported fluid scalar properties $\phi = h$, m_j, k, and ϵ) must be specified prior to solution. It is convenient now to consider the problem of closure of the equations.

B. Thermodynamic Relationships

Thermodynamic considerations provide some of the necessary extra equations to close the system; these may be

taken as

$$p=\rho RT/M \quad \text{where} \quad 1/M=\sum_j (m_j/M_j)$$

$$h=c_pT+\sum_j (H_jm_j)+v^2/2$$

R_j = provided by reaction model

$$\sum_j m_j=1 \tag{1}$$

where R is the universal gas constant, M is the mean mixture molecular weight which may be calculated from m_j and the molecular weight of species j, M_j, c_p is the mean mixture specific heat at constant pressure, and H_j is heat of combustion of species j.

Often consideration is given to a simplified main exothermic reaction between just two species, fuel *fu* and oxidant *ox*, combining with a stoichiometric oxidant/fuel ratio of i to form product *pr* plus release of energy. This and other assumptions lead to the simplifying equations:

$$1\ kg\ fu+i\ kg\ ox \rightarrow 1+i\ kg\ pr+H_{fu}$$

$$h=c_pT+H_{fu}m_{fu}+v^2/2$$

$$m_{fu}+m_{ox}+m_{pr}=1 \tag{2}$$

$$m_{ox}-im_{fu} \quad \text{is a conserved property}$$

Then solution for m_{fu}, $m_{ox}-im_{fu}$ and h enables a simple premixed chemical reaction to be simulated with the influence of chemical-kinetics included – fuel and oxidant may coexist at a point in the flow and the consumption rate of fuel $-R_{fu}$ is calculated depending on local specie concentrations, temperature and turbulence levels. For this one can use either the time-averaged Arrhenius model or eddy-breakup reaction model:

$$R_{fu}=-Pp^2m_{fu}m_{ox}\exp(-E/RT) \tag{3}$$

$$R_{fu}=-C_{EBU}\rho g^{1/2}\epsilon/k \tag{4}$$

where, in general and in SI units, $P=0.5$, $E/R=20{,}000.0$, and $C_{EBU}=0.53$ are constants for turbulent premixed flames of high temperature and high Reynolds numbers. The value of the latter model is that it tries to assert the effect of turbulence on the reaction, the time to heat up the premixed mixture by eddies of hot combustion product being related to the rate of dissipation of the fuel concentration. In many cases this is the limiting factor in controlling the reaction and not the final stages of molecular processes governed by an instantaneous Arrhenius expression. The variable g (mean square fluctuating component of fuel concentration) may be obtained from its governing equation or, with the assumption that generation equals dissipation, its reduced algebraic equation

$$g=(C_{g1}\mu\ k/C_{g2}\rho\ \epsilon)(\partial m_{fu}/\partial r)^2 \tag{5}$$

where $C_{g1}=3.0$ and $C_{g2}=0.132$. In the computations of Sec. IV., generally the lower of the two values from Eqs. (3) and (4) is used. Details may be found in a previous paper.[5]

C. Flux Laws

Turbulent flux vectors J_ϕ for transported fluid scalar properties ϕ may be described by the following generalized diffusion-flux law:

$$J_\phi=-\Gamma_\phi\nabla\phi \tag{6}$$

where the exchange coefficient Γ_ϕ may change its value with the direction of $\nabla\phi$, but the direction of J_ϕ is the exact opposite to that of $\nabla\phi$. If there is a diffusional component normal to this direction, it must be expressed as part of S_ϕ.

The turbulent transport of momentum is via the turbulent stress tensor τ, which cannot be expressed in so simple a manner as the transport of ϕ by diffusion; or rather it can but first the whole expression must be considered and only then transfer those unwanted components, which do not vanish in view of the continuity equation, into the source terms. The approximate expression is

$$\tau=2\mu\Delta \tag{7}$$

where μ is the turbulent viscosity and Δ is the time-mean flow rate of strain tensor, and again the value of μ may change according to which component of τ is under consideration.

The exchange coefficients μ and Γ_ϕ are connected to the other fluid properties such as density, temperature, composition, and turbulence characteristics by a variety of algebraic relations. If isotropy is assumed, often constant Prandtl, Schmidt and $r\theta$ (and other) viscosity numbers relate other exchange coefficients to the primary component of turbulent viscosity μ_{rx}; these are defined by

$$\sigma_\phi=\mu_{rx}/\Gamma_\phi \tag{8}$$

$$\sigma_{r\theta}=\mu_{rx}/\mu_{r\theta} \tag{9}$$

where often the former are taken near 0.7 and the latter as unity (isotropic). To describe the turbulent transport the two-equation k-ϵ turbulence model is to be used, whereby the turbulent viscosity is calculated from

$$\mu_{rx}=c_\mu\rho k^2/\epsilon \tag{10}$$

and two differential equations are solved for the two turbulence quantities k and ϵ. Constants appearing here and in Table 1 are given values recommended in Ref. 12: $c_\mu=0.09$, $c_D=1.00$, $c_1=1.44$, $c_2=1.92$, $\sigma_k=1.00$, and $\sigma_\epsilon=1.21$.

D. Common Form of the Governing Equations

All these linkages provide a high degree of nonlinearity in the total problem, and give the numerical analysis of fluid flow its peculiar difficulty and flavor. The above equations do not alone specify the problem; additional information of two

Table 1 The form of the source term in the general equation for ϕ, Eq. (11)[a]

ϕ	S_ϕ
u	$-\dfrac{\partial p}{\partial x}+S^u$
v	$-\dfrac{\partial p}{\partial r}+\dfrac{\rho w^2}{r}-\dfrac{\mu v}{r^2}+S^v$
w	$-\dfrac{\rho vw}{r}-\dfrac{w}{r^2}\dfrac{\partial}{\partial r}(r\mu)+S^w$
h	S^h
m_{fu}	R_{fu}
$m_{ox}-im_{fu}$	o
k	$G-c_D\rho\epsilon$
ϵ	$(c_1\epsilon G-c_2\rho\epsilon^2)/k$

[a] where $G=\mu[2\{(\dfrac{\partial u}{\partial x})^2+(\dfrac{\partial v}{\partial r})^2+(\dfrac{v}{r})^2\}$

$$+(\frac{\partial u}{\partial r}+\frac{\partial v}{\partial x})^2+\{r\frac{\partial}{\partial r}(\frac{w}{r})\}^2+(\frac{\partial w}{\partial x})^2]$$

kinds is needed: initial and boundary conditions for all the dependent variables. Details of this are given later in Sec. III. The similarity between the differential equations and their diffusion relations allows them all to be put in the common form

$$\frac{1}{r}\left\{\frac{\partial}{\partial x}(\rho u r\phi)+\frac{\partial}{\partial r}(\rho v r\phi)-\frac{\partial}{\partial x}\left(r\Gamma_\phi\frac{\partial\phi}{\partial x}\right)\right.$$

$$\left.-\frac{\partial}{\partial r}\left(r\Gamma_\phi\frac{\partial\phi}{\partial r}\right)\right\}=S_\phi \qquad (11)$$

i) ii) iii) iv) v)

for $\phi=u,v,w,h,m_{fu},m_{ox}-im_{fu},k$, and ϵ. The forms for the source term v are given in Table 1.

Now ϕ may stand for any of the velocity components, as well as for the other variables already mentioned; and, if ϕ is put equal to unity and Γ_ϕ and S_ϕ to zero, this equation stands also for the continuity equation. The difficulties to solution spring mainly from the interlinkages between the ϕ's. Those between the axial and radial velocity components are of a peculiar kind, each containing an unknown pressure gradient and the components are linked additionally by another equation, that of mass conservation, in which pressure does not appear. A successful solution procedure is one that takes account of these interactions and ensures that successive adjustments, which must be made to one variable after another, form an invariably convergent sequence. Details of the method now follow.

III. Solution Procedure

A. The Staggered Grid and Notation

Figure 1 shows some of the rectangular computational mesh. The intersections of the solid lines mark the grid nodes where all variables except the u and v velocity components are stored. The latter are stored at points which are denoted by the arrows and located midway between the grid intersections, and the boomerang-shaped envelopes enclose a triad of points denoted by a single letter $P=(I,J)$. Similar remarks apply also to the four neighbors $N=(I,J+1)$, $S=(I,J-1)$, $E=(I+1,J)$ and $W=(I-1,J)$. Thus, for example, $U_{I,J}=U(I,J)$ is the axial velocity at reference location (I,J) even though it actually represents the velocity positioned at $(I-\frac{1}{2},J)$. This grid arrangement has two special merits: first, it places the u and v velocities between the pressures that drive them and it is easy to calculate the pressure gradients that affect them; and second, these velocities are directly available for the calculation of the convective fluxes across the boundaries of the control volumes surrounding the grid nodes (see Sec. III. B). Those computer storage locations which appear to be external to the domain and its boundary (see Fig. 2) may be used to store the wall values of the appropriate variables. Boundaries are located midway between the mesh lines so that normal velocities are located directly on the boundaries; for example, u is located on a vertical boundary, and v on a horizontal one. Notice that there is no necessity for the distance between successive grid points to be uniform; frequently a gradually expanding rectangular mesh system is used on the grounds of accuracy and economy.

B. The Control Volumes

There are several possible ways in which finite difference equations can be derived; for example, Taylor series expansions, variational calculus, and integration over cell control volumes. There are good reasons why the third of these methods is preferred to the first two. It must be coupled with presumptions about the ways in which the variables are distributed between their locations; the presumptions are described in Sec. III.C.

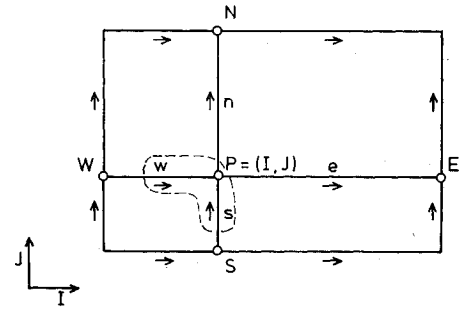

Fig. 1 Staggered grid and notation – three grids for p, w, etc. (o), for u velocity (→), and for v velocity (↑).

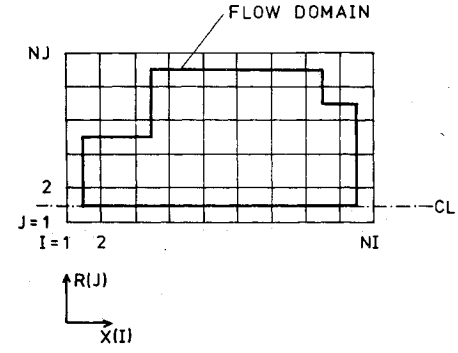

Fig. 2 Grid specification – an example of a rectangular domain being used with flow domain fitted inside.

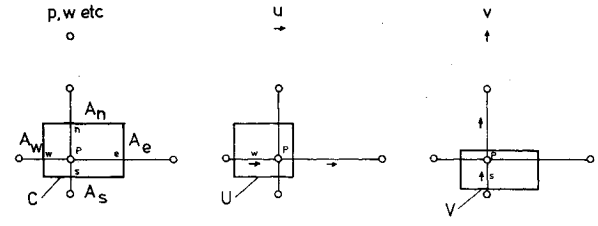

Fig. 3 Control volumes C, U, and V around each of the points P (o), w (→), and s (↑), respectively. Face areas are A_n, A_s, A_e, and A_w for C and similar for the U and V cells.

Figure 3 illustrates the control volumes enclosed by heavy lines that are employed. That marked C is employed when the variables at the 'o' points (P) are to be computed (for example, the balance of mass and of all ϕ's except u and v), while those marked U and V are used for computations of the axial and radial velocities u and v at the '→' (w) and '↑' (s) points, respectively. In each case control volume boundaries lie midway between successive locations of the variable in question.

Each control volume must not be thought of as an area. It is a volume going into the page a distance $r\delta\theta$ at any point located within the heavy boundary, where r is the distance from the axis of symmetry (cylindrical polar coordinates). The cell face area, the A's of Fig. 3, must take account of this and although $A_w=A_e$ note that $A_s\neq A_n$. Since the $\delta\theta$ occurs in all terms concerned with areas and volumes of the cells, it is supressed in the subsequent discussion and computer program.

C. The General Finite Difference Equations for ϕ

The discussion is now focused on the general dependent variable ϕ and its governing equation, Eq. (11). The finite difference equations are formed by integrating Eq. (11) over the control volume for the ϕ in question (see Fig. 3), and then expressing the resulting terms through gridpoint values. How the various terms in this equation are transformed is now described, assuming that ϕ is located at an 'o' point P with control volume marked C in Fig. 3.

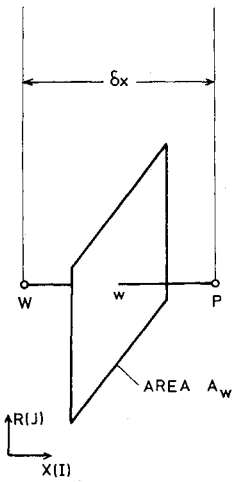

Fig. 4 One face of the control volume.

The term S_ϕ is integrated over the control volume by assuming that the values of ϕ and ρ at P prevail over the entire control volume C. Its volume integral is thus linearized to $S_P^\phi\ \phi_P + S_U^\phi$ where often S_P^ϕ is negative and aids the convergence of the iteration process. There is also a false source stabilizing trick which has no effect on the final solution obtained but alleviates situations that sometimes arise when mass flows at some stage do not satisfy continuity. Such situations sometimes yield all coupling coefficients to be zero and the finite difference equations to be singular. The trick is to add a false source of magnitude

$$S_{\text{false}} = |\dot{m}_{\text{net}}|\,(\phi_P^{\text{old}} - \phi_P) \tag{12}$$

where $\dot{m}_{\text{net}}$ is the net outflow of mass from a cell control volume at a certain stage in the computation.

When the convection and diffusion terms, labeled i-iv in Eq. (11), are integrated over the control volume, they give rise to the integral of the convective and diffusive fluxes across the control volume surfaces, via application of Gauss' divergence theorem. A proper representation of these terms is essential to the accuracy and convergence of the numerical procedure. Here is a 'hybrid' scheme, a combination of the so-called central and upwind differences. Its basis and some experiences with its use have been described;[20] it is also the scheme used in a widely-tested procedure for 2-D parabolic flows,[21] where the designation 'high-lateral flux modification' is used for it.

Consider the transport across one face of the control volume. Figure 4 shows the western face of area A_w normal to the x direction, which lies midway between the gridpoints W and P distant δx apart. The contribution C_w to the surface integral by this area A_w arises only from terms (i) and (iii) of Eq. (11) and is given by:

$$C_w = \begin{cases} (\rho u)_w A_w (\phi_W + \phi_P)/2 - (\Gamma_\phi)_w A_w (\phi_P - \phi_W)/\delta x \\ \qquad \text{for} \quad |Pe| < 2 \\ (\rho u)_w A_w \phi_W \quad \text{for} \quad Pe \geq 2 \\ (\rho u)_w A_w \phi_P \quad \text{for} \quad Pe \leq -2 \end{cases} \tag{13}$$

where $Pe = (\rho u)_w \delta x/(\Gamma_\phi)_w$ is a cell Peclet number calculated at the western face of the cell. When the relative magnitude of convection is small (corresponding to the absolute value of Pe being less than 2), the formula implies a linear variation of ϕ between the gridpoints W and P. When the convection rate is large the diffusion is put equal to zero and the ϕ value of the material crossing the face is taken as that prevailing at the gridpoint on the upstream side of the face.

When the integrals of the various terms in Eq. (11) are expressed in the manner described above, the following general equation is obtained:

$$a_P^\phi\ \phi_P = \sum_j a_j^\phi\ \phi_j + S_U^\phi \tag{14}$$

where

$$a_P = \sum_j a_j^\phi - S_P^\phi$$

$$\sum_j = \text{sum over N, S, E, and W points}$$

$$\iiint_V S_\phi dV = S_P^\phi\ \phi_P + S_U^\phi$$

D. The Finite Difference Equations for u and v

The finite difference equations for u and v are obtained in a similar manner, but there are two points of difference. First, the control volumes will be around the points indicated by arrows in Fig. 3, and second, a part of the source term will contain the difference in pressure between two neighboring gridpoints. Thus, the difference equation for u will have the form

$$a_P^u\ u_P = \sum_j a_j^u u_j + S_U^u + A_w (p_W - p_P) \tag{15}$$

where the notation is as for Eq. (14) above and remembering that u velocity locations are actually displaced to the left of their designated subscripts (see Fig. 1). Since the values of pressure p appearing in Eq. (15) are not known, when we wish to use this equation, it is our practice to substitute the best estimate so far of the pressure field denoted by p^* into Eq. (15) and so obtain a preliminary velocity field u^* and v^*. Thus

$$a_P^u u_P^* = \sum_j a_j^u u_j^* + S_U^u + A_w (p_W^* - p_P^*) \tag{16}$$

The true pressure p is related to the estimate pressure p^* by

$$p = p^* + p' \tag{17}$$

where p' is the so-called pressure correction. We further suppose that the true velocity u is connected to u^* via the approximate relation

$$u_P = u_P^* + D^u (p'_W - p'_P) \tag{18}$$

where $D^u = A_w/a_P^u$. A similar equation can be derived for v. How to obtain the pressure correction p' is described in the following.

E. Poisson Equation for Pressure

The equation for p', to be derived below, is just a new form of what is known in the literature as the Poisson equation for pressure. It is derived by combination of the momenta and continuity equations. The preliminary velocity fields of u^* and v^* will not in general satisfy the continuity equation, Eq. (1). The pressure corrections are therefore applied such that the velocity field is brought into conformity with this equation. The finite difference form of the continuity equation is

$$(\rho u)_w A_w - (\rho u)_e A_e + (\rho v)_s A_s - (\rho v)_n A_n = 0 \tag{19}$$

where the A's are the areas of the $n,s,e,$ and w faces of the control volume C around P; see Fig. 3. Assuming the density does not depend on pressure, it can be calculated from the values of other variables. Then, substituting from equations

like Eq. (18) into Eq. (19), the following equation for p' is obtained:

$$a_P^p\, p'_P = \sum_j a_j^p p'_j + S_U^p \tag{20}$$

where

$$a_P^p = \sum_j a_j^p$$

$\sum_j$ = sum over N, S, E, and W neighbors

S_U^p = term which results from mass sources of u^* and v^* fields

F. Boundary Conditions

The above discussion has shown how finite difference equations are prepared for a general variable ϕ, for the u and v velocity components and for the pressure correction. All these equations have the same form, namely that the value of a variable at a location is conncected to its value at its four neighboring locations and a source term. Its connecting coefficients and source term involve other variables and give the equations a strong coupling, requiring an iterative solution procedure. A prerequisite for this is that values of dependent variables at boundaries of the region of integration must be specified. The only novelties concern the boundary conditions on the pressure and velocity components – the other variables may be handled in the usual ways.

Usually either the velocities or pressures are known at the boundaries. When it is the former, no special difficulty arises, for these velocities act in the usual fashion. In the pressure correction equation, they usually enforce zero normal gradient conditions on p' via Eq. (18), for example. When it is the latter that are given at the boundaries, then $p = p^*$ and $p' = o$ at the boundary, and there is some deliberation about what conditions to impose on the boundary velocities. When the boundary is one of outflow, the velocity at it may be adjusted proportionally at each iteration so as to ensure overall mass conservation as compared with the inlet flow. At inflow boundaries of prescribed pressure, the near-boundary normal velocity must be deduced in a different way. The Bernoulli equation, which connects the velocity at a grid point with the mean of neighboring pressures, is then used in a linearized form to procure convergence. The details are in Ref. 12.

G. Solution Procedure

The finite difference equations and boundary conditions constitute a system of strongly-coupled simultaneous algebraic equations. Though they appear linear they are not, since the coefficients and source terms are themselves functions of some of the variables and the velocity equations are strongly linked through the pressure. The solution proceeds by the cyclic repetition of the following steps: 1) guess the values of all variables including p^*; hence calculate auxiliary variables like density, viscosity etc.; 2) solve the axial and radial momentum equations to obtain u^* and v^* from equations like Eq. (16); 3) solve the pressure correction equation, Eq. (20), to obtain p'; 4) calculate the pressure p and the corrected velocities u and v from Eq. (17) and equations like Eq. (18), respectively; 5) solve the equations like Eq. (14) for the other ϕ's successively; and 6) treat the new values of the variables as improved guesses and return to step 1. Repeat the process until convergence.

In the solution procedure, algebraic equations like Eq. (14) are solved many times, coefficient and source updating being carried out prior to each occasion. How is a set of such equations, one for each grid point, for a particular ϕ to be solved each time? There are three possibilities. One may treat each equation as an equation for ϕ_p directly in terms of previous values of ϕ at its four neighboring locations $N,S,E,$ and W – an explicit procedure of the Gauss-Seidel variety with its well-known limiations. Alternatively one may think of each equation as a relationship between five unknowns, the values of ϕ at P,N,S,E and W. Then a set of n simultaneous equations (where n is the total number of grid points), each containing five unknowns, must be solved at each iteration stage (for particular values of coefficients and source term). Thus some relaxation procedure with several iterations must be employed to obtain some degree of convergence prior to property updating. The complete procedure tends to be lengthy. The practice used here is to make use of the well-known tridiagonal matrix algorithm (TDMA), whereby a set of equations, each with exactly three unknowns in a particular order except the first and last, which have exactly two unknowns, may be solved sequentially. In the 2-D problem one considers the values at gridpoints along a vertical gridline to be unknown (values at $P,N,$ and S for each point P), but take as known, most recent values being used, the values at each E and W neighbor. The TDMA is then applied to this vertical gridline. In this manner one can traverse along all the lines in the vertical direction sequentially from left to right of the integration domain. In a given iteration it is not essential to obtain an accurate solution of the algebraic equations, because the coefficients in these equations are only tentative and must be updated prior to the next iteration, and usually only one or two traverses is sufficient. This so-called line-by-line (LBL) solution procedure has been found to be particularly effective in solving elliptic problems.[12]

In deciding about convergence, rather than use the well-established fractional-change criterion, which is a necessary but not sufficient criterion for convergence, the current practice is to use the residual-source criterion. The residual sources are defined for each variable, at each point at each iteration, by equations like

$$R_P^\phi = a_P^\phi \phi_P - \sum_j a_j^\phi \phi_j - S_U^\phi \tag{21}$$

which has been obtained from Eq. (14) and which measures the departure from exactness (except for the use of current coefficients and source) for the variable ϕ at the point P. When each of these quantities becomes smaller than a certain fraction of a reference value, the finite difference equations are declared to be solved.

The process described in Sec. III. G, frequently procures convergence without further refinement. More often, however, it is necessary to employ some degree of underrelaxation, for example when solving equations like Eqs. (14), (16) and (20), to take a weighted average of the newly calculated value and the previous value at each point. In updating properties like density, viscosity and fuel source term R_{fu}, similar underrelaxing is often used. This practice is helpful in combating the influence of the variations of the coefficients from cycle to cycle, but it is not an infallible technique that would invariably ensure convergence since the equations are nonlinear.

IV. Sample Computations

Whereas the main interest is on the application of the code just described to gas turbine combustors, the emphasis here is on free or confined flows, with or without chemical reaction, downstream of sudden expansions of the axisymmetric cross-sectional area. The effect of strong swirl on such flows has previously been described, modeled, and predicted with a stream function-vorticity technique and a simple algebraic turbulence model.[7] There is no need here to duplicate that description of the interesting effects of swirl on flowfields, but, as examples of current predictive capability with the present technique, two sets of computations are now discussed

representing a free swirling jet from a swirl generator and an enclosed swirling premixed flame from swirl vanes. For comparison purposes, it is worth noting that vane angle ϕ and swirl number S are related approximately by

$$S \approx \tfrac{2}{3} \tan\phi \qquad (22)$$

for $d_h \ll d$ so that vane angles of 15, 30, 45, and 60, for example, correspond to S values of 0.179, 0.385, 0.667, and 1.155.

Computations made with a 20×20 grid allowed the solution of a typical swirling reacting problem in about 9 min of CDC 6600 CP time; though, in the generation of results for successively stronger degrees of swirl, previous solution values in the field for a weaker degree of swirl were used as initial values for the next more strongly swirling case. Underrelaxation parameters were set to be less effective as the iteration procedure for a particular problem nears convergence. Thus their initial stabilizing effect does not hinder the final convergence rate.

A. Strongly Swirling Free Jets

A tangential and axial entry swirl generator gives a strongly swirling flow but with exit u and v velocities progressing peaked toward the outer edge of the nozzle as the swirl number S increases. As S increases the w profile tends to be more peaked than solid body rotation and the u profile ensures that much of the flow leaves near the outer edge. Such a flow, expanding into free air, has been investigated experimentally[22] in the presence of a central hub of diameter $d_h = 0.24d$ in a swirl generator of exit diameter $d = 0.254$ m. The mean exit velocity $u_{av,o}$ averaged 10 m/s and the effect of the degree of swirl on the size and shape of the recirculation zone and the decay of axial and swirl velocities were studied.

The axial and swirl velocities decay more rapidly with increased swirl. Station maxima at $z/d = 2$ are shown in Fig. 5, and these compare well with the experimental evidence. The velocities both decay more rapidly with higher values of swirl when compared with their initial peaked values, but the effect is less dramatic when they are compared with average exit velocity values. The effect is still there, however, manifesting itself also in a wider, slower jet flow where radial and axial pressure gradients become increasingly important.

There is always at least a small central recirculation zone because of the central hub and the jet flow in the surrounding annulus. Its length progressively increases, though, as the degree of swirl, together with the axial pressure gradient, increases. The general trend, as discussed previously,[7] may be predicted also by the present technique. As an example, predicted streamlines and recirculation zone for the $S = 1.5$ jet show striking resemblance to the experimental figure,[22] but the zone is predicted slightly too wide and too short (Fig. 6).

B. Strongly Swirling Enclosed Premixed Flames

Plug flow in an annulus of outer and inner diameters d and d_h passes over swirl vanes at angle ϕ to the axis, imparting a flat w profile on the flow that then enters a sudden expansion into a cylindrical chamber of diameter D and length L. In the experiment[23] $d = 0.098$ m, $d_h = 0.33d$, $D = 5d$, and $L = 15d$. The flow consisted of premixed town gas with air and the gas may be taken as $m_{fu} = 0.0625$, $M_{fu} = 14$, $H_{fu} = 26{,}600{,}000.0$ J/kg and stoichiometric ratio (oxygen/fuel) $i = 3.5$. Chemical reaction ensued downstream of the vane swirler and the study involved observing the effect of the swirl vane angle ϕ on axial and swirl velocities, temperature and central recirculation zone. For the theoretical simulation, walls are taken to be adiabatic, exit flow is assumed parallel, and turbulence and reaction models as described in Sec. II are used.

Results show in general that increasing the vane angle ϕ produces a shorter wider flame with greater combustion intensity and hastens the decay of axial and swirl velocities. The form of the results depends on whether or not a central recirculation zone is established and, both in theory and practice, this is found to be for ϕ greater than 30°. With weak swirl and no recirculation, increasing the vane angle increases the jet spread in a similar fashion to that observed in free-burning jet flows.[5] With recirculation present at the larger vane angles, the jet spread is considerably more rapid than in a corresponding free flame case.

Figure 7 shows the predicted and experimental effect of swirl vane angle ϕ on the length of the central recirculation zone and the flame length. It is seen that as ϕ increases above 30° there is a rather sudden occurrence of recirculation zone whose length remains constant for larger vane angles. The agreement is satisfactory, though slightly underpredicted as in the previous section. Streamlines and recirculation zone boundaries are similar to those for nonreacting flow shown in Fig. 6. As swirl increases, turbulence increases and the central recirculation zone appears resulting in a shorter flame length.

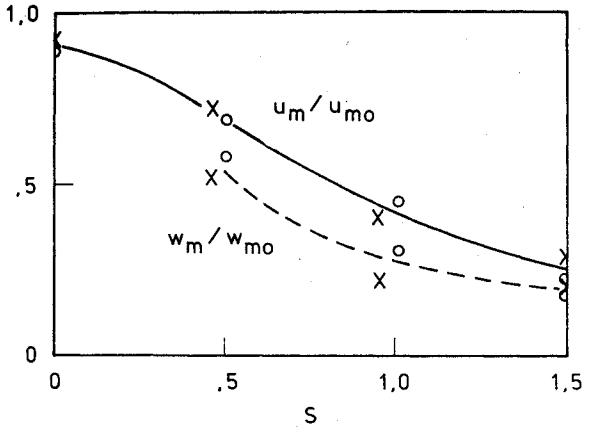

Fig. 5 Effect of swirl on axial (—) and swirl (----) velocity values at $z/d = 2$ (X = experiment, o = predicted).

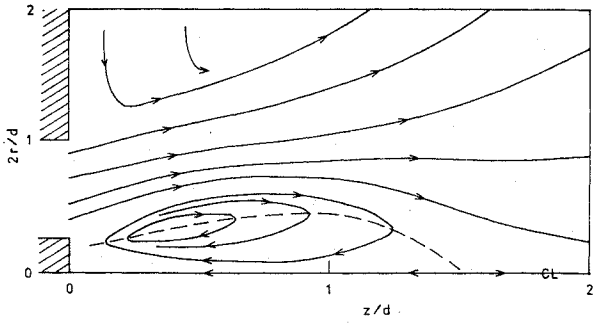

Fig. 6 Predicted streamlines (—) and recirculation zone (----) for $S = 1.5$ jet.

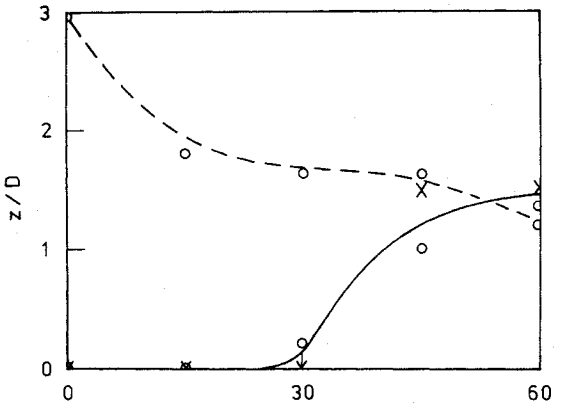

Fig. 7 Effect of swirl vane angle ϕ on the central recirculation zone length (—) and flame length (----) (X = experiment, o = predicted).

Both these effects are well-known to combustion engineers,[1] who strive to utilize the recirculation of hot combustion products and the bluff body effect of this zone as an aid to the combustion process. The more rapid burning of fuel allows a greater length of mixing region, where hot combustion products are able to mix freely with cooler air, and improves the temperature traverse quality (a measure of the uniformity of temperature) at the exit from the system. All these trends are in conformity with expectations based on observations and previous predictions of a swirling diffusion flame confined in an idealized combustion chamber.[7]

V. Conclusions

A new primitive pressure-velocity finite difference technique has been presented in a form suitable for the prediction of strongly swirling recirculating flows. The method and program involve a staggered grid system for axial and radial velocities, a line relaxation technique for efficient solution of the equations and a two-equation k-ϵ turbulence model, together with a simple one-step chemical reaction model based on eddy-breakup concepts. Finite difference predictions are now possible by this means of inert and reacting axisymmetric turbulent flows, showing the effect of swirl on jet growth, entrainment, and decay and flame size, shape, and combustion intensity, as well as the occurrence of a central toroidal recirculation zone at high degrees of swirl. Predictions of this type allow some results to be obtained more cheaply, quickly, and correctly than currently possible by the almost exclusive use of experimental means. Further development and application is providing a valuable supplementary technique for designers of practical combustion equipment.

References

[1] Beer, J. M. and Chigier, N. A., "Combustion Aerodynamics," *Applied Science*, London, 1972.

[2] Roache, P. J., *Computational Fluid Dynamics*, Hermosa, Albuquerque, N. Mex., 1972.

[3] Lilley, D. G., "Numerical Solution of Turbulent Swirling Flows," Paper presented at IMA Conf. on Computational Methods and Problems in Aeronautical Fluid Dynamics, Manchester, England, Sept. 1974, Proceedings, Academic Press, London, 1976.

[4] Lilley, D. G., "Prediction of Inert Turbulent Swirl Flows," *AIAA Journal*, Vol. 11, July 1973, pp. 955-960.

[5] Lilley, D. G., "Turbulent Swirling Flame Prediction," *AIAA Journal*, Vol. 12, Feb. 1974, pp. 219-223.

[6] Lilley, D. G., "Modeling of Combustor Swirl Flows," *Acta Astronautica*, Vol. 1, No. 9, 1974, pp. 1129-1147.

[7] Lilley, D. G., "Swirl Flow Modeling for Combustors," AIAA Paper 74-527, Palo Alto, Calif., 1974.

[8] Lilley, D. G., "Combustor Swirl Flow Modeling," *AIAA Journal*, Vol. 13, April 1975, pp. 419-420.

[9] Gosman, A. D., Pun, W. M., Runchal, A. K., Spalding, D. B., and Wolfshtein, M. W., *Heat and Mass Transfer in Recirculation Flows*, Academic Press, London, 1969.

[10] Patankar, S. V. and Spalding, D. B., "A Calculation Procedure for Heat, Mass, and Momentum Transfer in Three-Dimensional Parabolic Flows," *International Journal of Heat Mass Transfer*, Vol. 15, 1972, pp. 1787-1806.

[11] Patankar, S. V. and Spalding, D. B., "Numerical Prediction of Three-Dimensional Flows," Report HTS/72/4, Dept. of Mechanical Engineering, Imperial College, London, 1972.

[12] Gosman, A. D. and Pun, W. M., Lecture Notes for course entitled "Calculation of Recirculating Flows," Report HTS/74/2, Dept. of Mechanical Engineering, Imperial College, London, 1974.

[13] Patankar, S. V., "On Available Calculation Procedures for Steady Three-Dimensional Boundary Layers," Report HTS/71/38, Dept. of Mechanical Engineering, Imperial College, London, 1971.

[14] Harlow, F. H., "Numerical Methods for Fluid Dynamics, an Annotated Bibliography," Report LA-4281, Los Alamos Scientific Laboratory, Los Alamos, N. Mex., 1969.

[15] Harlow, F. H. and Welch, J. E., "Numerical Calculation of Time-Dependent Viscous Incompressible Flow of Fluid with Free Surface. (The MAC Method)," *Physics of Fluids*, Vol. 8, 1965, pp. 2182-2189.

[16] Amsden, A. A. and Harlow, F. H., "The SMAC Method: A Numerical Technique for Calculating Incompressible Fluid Flows," Report LA-4370, Los Alamos Scientific Laboratory, Los Alamos, N. Mex., 1970.

[17] Chorin, A. J., "A Numerical Method for Incompressible Viscous Flow Problems," *Journal of Computational Physics*, Vol. 2, 1967, pp. 12-26.

[18] Caretto, L. S., Curr, R. M., and Spalding, D. B., "Two Numerical Methods for Three-Dimensional Boundary Layers," *Computation Methods in Applied Mechanics and Engineering*, Vol. 1, 1972, pp. 39-57.

[19] Caretto, L. S., Gosman, A. D., Patankar, S. V., and Spalding, D. B., "Two Calculation Procedures for Steady Three-Dimensional Flows with Recirculation," *Proceedings of the 3rd International Conference on Numerical Methods in Fluid Mechanics*, Vol. 2, J. Ehlers, K. Hepp and H. A. Weidenmüller, eds., Springer-Verlag, Germany, 1973, pp. 60-68.

[20] Spalding, D. B., "A Novel Finite-Difference Formualtion of Differential Expressions Involving Both First and Second Derivatives," *International Journal of Numerical Methods in Engineering*, Vol. 4, 1972, pp. 551-559.

[21] Patankar, S. V. and Spalding, D. B., *Heat and Mass Transfer in Boundary Layers*, 2nd ed., Intertext, London, 1970.

[22] Chigier, N. A. and Beer, J. M., "Velocity and Static-Pressure Distributions in Swirling Air Jets Issuing from Annular and Divergent Nozzles," *Journal of Basic Engineering*, Vol. 86, No. 4., Dec. 1964, pp. 788-798.

[23] Beltagui, S. A. and Maccallum, N. R. L., "Aerodynamics of Swirling Flames – Vane Generated Type," *Proceedings of the Combustion Institute, European Symposium* (Weinberg, F. J., ed.), Academic Press, London, 1973, pp. 559-564.